Research Article

Journal of Environmental Nanotechnology

Facile Synthesis, Characterisation, and Catalytic Application of Lipase Immobilized Nickel Oxide Nanoparticles for Biodiesel Production

Jeevitha Parthiban[1] and J. Ranjitha[2*]

[1]Department of Chemistry, School of Advanced Sciences, Vellore Institute of Technology, Vellore, TN, India
[2]CO_2 Research and Green Technologies Centre, Vellore Institute of Technology, Vellore, TN, India
Received: 26.06.2025 Accepted: 26.08.2025 Published: 30.09.2025
*jranji16@gmail.com

ABSTRACT

The growing global demand for clean and sustainable energy has prompted researchers to focus on producing biodiesel using enzymes. In this study, nickel oxide (NiO) nanoparticles were prepared using a sol-gel method and modified to attach lipase enzymes. The resulting nanobiocatalyst was analysed using X-ray diffraction (XRD), Fourier-transform infrared spectroscopy (FTIR), and scanning electron microscopy (SEM) to investigate its size, shape, and enzyme attachment. Lipase from *Candida albicans* was bonded to the NiO particles through covalent linking. This enzyme-nanoparticle system was tested for its ability to convert waste cooking oil into biodiesel. Reaction settings were optimised to achieve the best yield, and the catalyst's ability to be reused was also investigated. Under ideal conditions, the process yielded 88% biodiesel and retained more than 75 % activity even after five uses. These results demonstrate that lipase-bound NiO nanoparticles can serve as a highly effective and reusable catalyst for the production of green biodiesel.

Keywords: Lipase immobilised nickel oxide nanoparticles; Nanobiocatalyst; Biodiesel; Transesterification.

1. INTRODUCTION

The depletion of fossil fuels and environmental concerns have driven the search for renewable energy alternatives. Firstly, there are significant fluctuations in fossil fuel prices, with increases of more than 5–7 times over short periods, and at times even dropping to negative values (Foster *et al*. 2017; Chen *et al.* 2019). Secondly, the use of fossil fuels has severe environmental consequences, contributing to climate change and global warming (Binsted, 2022; Mercure *et al.* 2021). Biofuels, including bioethanol, biodiesel, and biogas, are emerging as promising alternatives to help meet future energy demands (Basumatary *et al.* 2018). Over the past two decades, biodiesel has emerged as a potent substitute for fossil fuels due to its comparable properties to petrodiesel (Nath *et al*. 2019). The use of bioenergy, particularly biofuels, is considered one of the most promising renewable energy alternatives (Cherubini and Strømman, 2011), mainly due to their cost-effective synthesis methods (Singh *et al.* 2021). Biodiesel, derived from renewable sources such as vegetable oils and animal fats, has gained attention due to its biodegradability, lower emissions, and sustainability. Among various biofuels, biodiesel has garnered significant research interest because of its numerous advantages over conventional fossil fuels and the flexibility in feedstock selection. Key benefits of biodiesel include being sulfur-free, having adequate oxygen content, a relatively simple manufacturing process, and significantly reduced greenhouse gas (GHG) emissions (Tayari *et al.* 2020). Moreover, biodiesel is biodegradable (Okoye *et al.* 2019), non-toxic (Garcia *et al.* 2020), portable, and environmentally sustainable (Sun and Li, 2020), and exhibits high efficiency with low sulfur and aromatic content (Esmaeili, 2022). Its higher flash point also makes biodiesel safer to transport and store compared to traditional diesel fuels.

Biodiesel, commonly known as fatty acid methyl esters (FAME), can be chemically produced from a variety of feedstocks, including edible oils, non-edible oils, waste cooking oil (WCO), animal fats, and microalgal lipids. This production typically occurs through esterification or transesterification reactions with short-chain alcohols, such as methanol or ethanol (Gui *et al*. 2008; Rawat *et al*. 2013; Sharma and Singh, 2009). Methanol is the most commonly used alcohol in biodiesel synthesis due to its low cost, reactivity, and favourable green chemistry metrics (Koberg *et al.* 2011; Guerra and Gude, 2017; Borges and Díaz, 2012; Serio *et al.* 2008; Ramadhas *et al*. 2005; Majhi, 2025). Enzymatic transesterification, particularly using lipase enzymes, offers advantages over chemical catalysis, including milder reaction conditions and reduced byproducts (Agarwal *et al.* 2022; Parthiban and Jambulingam, 2023). Nanoparticles have gained significant attention in enzymatic transesterification processes due to their high

surface area, enhanced enzyme immobilisation efficiency, and ability to improve catalytic performance and reusability in biodiesel production. Free enzymes and immobilised enzymes are used for the enzymatic transesterification reaction. Compared to free enzymes, immobilised enzymes are more stable. However, free enzymes often suffer from low operational stability and poor reusability, making the process economically unviable. Nanoparticle-based immobilisation of enzymes addresses these limitations by enhancing enzyme stability, activity, and reusability. Nickel oxide nanoparticles (NiO NPs) have emerged as promising supports due to their high surface area, chemical stability, and potential magnetic properties, which facilitate easy recovery and separation (Abukhadra *et al.* 2019; Rajendran *et al.* 2018). This study focuses on synthesising NiO nanoparticles, immobilising lipase, characterising the resulting nanobiocatalyst, and evaluating its efficacy in biodiesel production from algal oil.

2. MATERIALS AND METHODS

2.1 Materials

Nickel nitrate hexahydrate ($Ni(NO_3)_2 \cdot 6H_2O$), sodium chloride, EDTA, EDC, sodium taurocholate, sodium hydroxide, deionised water, nickel hydroxide, APTES (3-aminopropyl) triethoxysilane, N-hydroxysuccinimide (NHS), ethanol, and chloroform were purchased from SD Fine Chemicals. All other chemicals and solvents were of analytical grade and used without further purification.

2.2 Synthesis of Nickel Oxide Nanoparticles

Initially, 16.5 g of $Ni(NO_3)_2 \cdot 6H_2O$ was dissolved in 120 mL of deionised water and stirred for 15 minutes to obtain a homogeneous green-colored solution (Solution A). Separately, 16 g of NaOH was dissolved in 250 mL of deionised water to prepare an alkaline solution (Solution B). Solution B was added dropwise to Solution A using a burette under constant magnetic stirring at 75 °C and 300 rpm. The pH of the reaction mixture was adjusted to 12, leading to the formation of a green precipitate of nickel hydroxide. The resulting suspension was filtered to collect the precipitate, which was then dried in a hot-air oven at 400 °C for 4 hours, with a controlled heating rate of 3–5 °C/min. After drying, a fine black NiO powder was obtained and used for further characterization (Kalita *et al*. 2022; Teouqeer *et al*. 2021).

2.3 Lipase Immobilization of Nickel Oxide Nanoparticles

To prepare NiO-APTES nanoparticles, 0.25 g of NiO nanoparticles was dispersed in 4.85 mL of ethanol, followed by the addition of 0.15 mL of APTES. The mixture was sonicated overnight at room temperature at a frequency of 35 kHz. The resulting product was separated by magnetic separation, washed with 5% ethanol to remove unbound residues, and then dried in an oven at 50 °C. For lipase immobilisation, 10 mg/mL of lipase solution was mixed with 0.5 mL of EDC solution (2.5 mg/mL) and shaken at 200 rpm for 2 hours at room temperature. Then, 3 mg of N-hydroxysuccinimide (NHS) was added to the mixture, which was then incubated for an additional 2 hours under the same conditions. Subsequently, 0.25 g of NiO-APTES nanoparticles was added to the reaction mixture and incubated for an additional 2 hours to facilitate covalent bonding. After activation of the reaction, the lipase-immobilised NiO nanoparticles were separated *via* magnetic decantation, thoroughly washed with distilled water to remove unbound enzyme, air-dried, and stored at 4 °C for further studies (Xie and Ma, 2010).

2.4 Characterisation Techniques

The structural and morphological properties of the synthesised and immobilised nanoparticles were characterised as follows: X-ray diffraction (XRD) measurements were performed using a LynxEye detector and a PMMA sample holder. The scans were conducted at a speed of 1°/mm per second with a step size of 0.01°, covering a 2θ range from 10° to 80°. A Cu Kα radiation source with Ni-filtered light was used to determine the X-ray wavelength. Fourier-transform infrared (FTIR) spectroscopy was carried out using a Nicolet 510 FTIR analyser equipped with a DTGS detector. The spectra were recorded with a resolution of 2 cm^{-1} over the range 4000–400 cm^{-1}. Potassium bromide pellets were used for the measurements. The SEM imaging was performed using a Carl Zeiss SUPRA 55 field-emission scanning electron microscope (FE-SEM) operated at an accelerating voltage of 5 kV (Jambulingam *et al.* 2019; Joghee *et al*. 2018).

2.5 Biodiesel Production and Catalytic Evaluation

The lipid extract from *Synechococcus elongatus* was initially treated with methanol at a molar ratio of 4:1 (methanol to lipid). Subsequently, 250 mg of the nanobiocatalyst was added to the reaction mixture, along with 25 mL of n-hexane, serving as the organic solvent. The mixture was stirred using a magnetic stirrer at 45 °C for approximately 4 hours to facilitate transesterification. After the reaction, the mixture was washed with 25 mL of chloroform to facilitate phase separation. The organic layer containing the biodiesel was then separated and further washed with deionised water to remove any residual impurities or byproducts (Xie and Ma, 2010; Padilha *et al*. 2012). Samples were withdrawn periodically and analysed for biodiesel content using gas chromatography. The effects of reaction parameters, such

as the methanol-to-oil ratio, enzyme concentration, temperature, and reaction time, were optimised to achieve the maximum yield.

2.6 Reusability and Storage Stability Test

The stability of the immobilised enzyme was evaluated through repeated reaction cycles. After each enzymatic run, the immobilised nanoparticles were magnetically separated, rinsed with hexane, and then with deionised water to remove residual substrate. Their hydrolytic activity in olive oil was subsequently measured. To assess storage stability, both free and immobilised lipase samples were stored at pH 7.0 and 4 °C for 100 days. Enzymatic activity was measured at 10-day intervals using a titration method, and the relative activity was recorded to monitor changes over time. To assess the reusability of the immobilised enzyme, the nanobiocatalyst was separated after each reaction cycle by centrifugation, washed with phosphate buffer, and reused under identical conditions. The residual activity and biodiesel yield were measured after each cycle.

3. RESULTS AND DISCUSSION

3.1 Characterisation of Nickel Oxide Nanoparticles

3.1.1 X-ray Diffraction (XRD) Analysis

Powder X-ray diffraction was employed to evaluate the crystallinity and phase purity of the synthesised NiO nanoparticles, as illustrated in Fig. 1. The prominent diffraction peaks observed at 2θ values of 37.20°, 43.20°, 62.87°, 75.20°, and 79.38° correspond to the (111), (200), (220), (311), and (222) crystal planes, respectively. These reflections can be precisely indexed to the face-centered cubic (FCC) structure of NiO, as specified in the standard JCPDS card No. 001-1239. The close agreement between the observed diffraction pattern and the standard reference, both in peak positions and relative intensities, indicates that the synthesised NiO nanoparticles exhibit high crystallinity and phase purity. Similar diffraction peaks were also observed in the lipase-immobilised NiO nanoparticles, confirming that the immobilisation process did not alter the fundamental crystalline structure of NiO. This observation is consistent with previous reports (Niasari *et al.* 2012; Vatanparast *et al*. 2014). The average crystallite size was calculated using the Debye–Scherrer equation and found to be in the range of 20–40 nm. These results confirmed the successful synthesis of crystalline NiO nanoparticles.

3.1.2 Fourier-transform Infrared Spectroscopy (FTIR)

The FTIR spectrum of chemically synthesised NiO nanoparticles is shown in Fig. 2. A broad absorption band observed at 3308 cm^{-1} is attributed to the O–H stretching vibrations of interlayer water molecules and hydrogen-bonded hydroxyl groups present on the surface of NiO nanoparticles (Song and Gao, 2008). The absorption peak at 1028 cm^{-1} corresponds to the bending vibrations of C–H bonds, while the peak at 1400 cm^{-1} is associated with the bending and stretching vibrations of hydroxyl groups (Wongsaprom and Maensiri, 2013). A distinct peak at 1556 cm^{-1} is assigned to C=C stretching vibrations (Ali *et al*. 2013). Notably, strong absorption bands observed in the range of 600–700 cm^{-1} indicate the presence of Ni–O bonds, confirming the successful synthesis of NiO nanoparticles. In particular, the peaks at 605 cm^{-1} and 672 cm^{-1} are characteristic of Ni–O stretching vibrations (Wang *et al*. 2005).

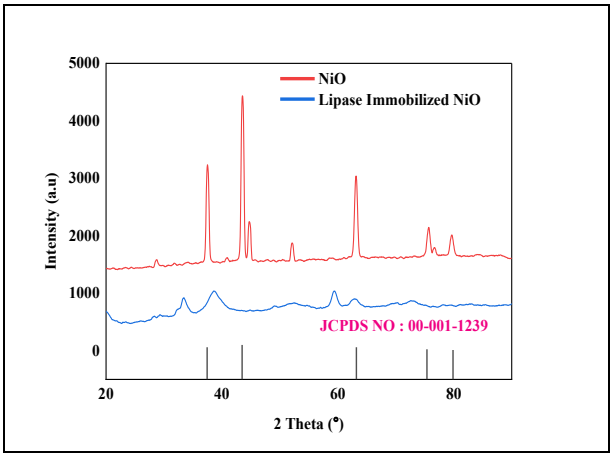


Fig. 1: XRD of NiO nanoparticles

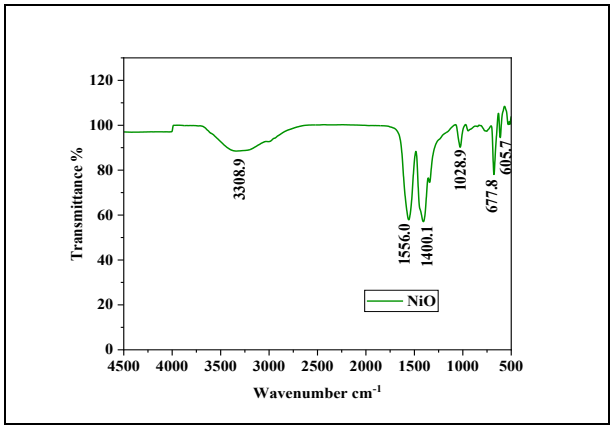


Fig. 2: FTIR of NiO nanoparticles

3.1.3 Scanning Electron Microscopy (SEM)

The SEM images revealed that the NiO nanoparticles had a relatively uniform spherical morphology with slight agglomeration (Fig. 3). The SEM images reveal that the synthesised nanoparticles possess a uniform spherical morphology with smaller, randomly distributed grains. It is also evident that the enzyme is successfully coated on the outer surface of the nanoparticles, indicating effective surface functionalisation and immobilisation.

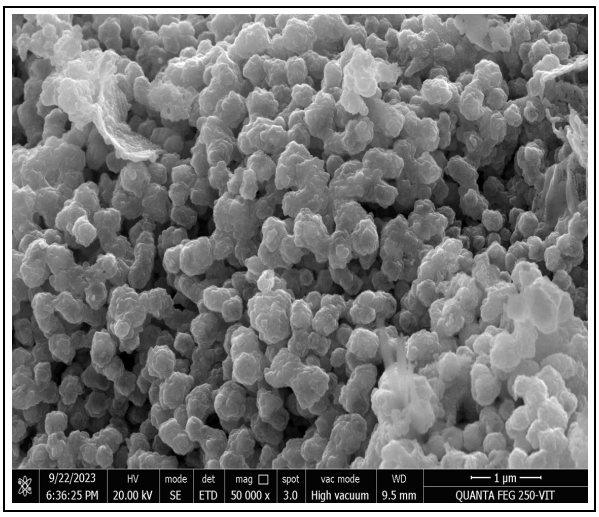


Fig. 3: SEM image of NiO nanoparticles

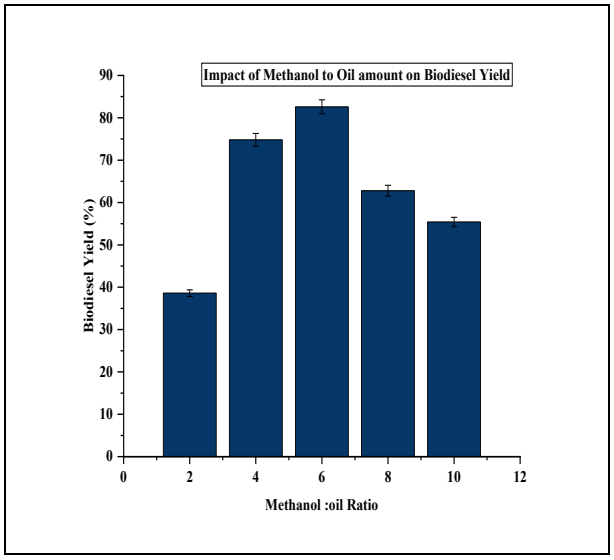


Fig. 4: Effect of methanol-to-oil ratio

3.2 Evaluation of Catalytic Activity in Biodiesel Production

3.2.1 Optimisation of Reaction Conditions

The transesterification of algal oil using the immobilised lipase was optimised by varying key parameters:

3.2.1.1 Effect of Methanol-to-oil Ratio

A 6:1 molar ratio was found optimal; higher ratios led to lipase inhibition (Fig. 4). Methanol plays a crucial role in biodiesel production through the transesterification reaction, serving as a key parameter that influences the process's efficiency. The choice and volume of methanol significantly affect the feasibility of the response, particularly by controlling the solubility and dispersion of the catalyst (Muthukumaran *et al.* 2017). In this study, the maximum biodiesel yield achieved was 88.6 %.

3.2.1.2 Effect of Temperature

Temperature is a crucial parameter that influences the efficiency of enzymatic transesterification reactions. To evaluate its impact on biodiesel yield, the reaction temperature was varied from 50 °C to 70 °C in 5 °C increments (Fig. 5). The reactions were conducted at a constant stirring speed of 400 rpm, with a methanol-to-oil molar ratio of 6:1, for approximately 6 hours. The highest biodiesel yield was obtained at 60 °C, with a maximum fatty acid methyl ester (FAME) conversion of roughly 88 %. The activity declined above 70 °C due to enzyme denaturation.

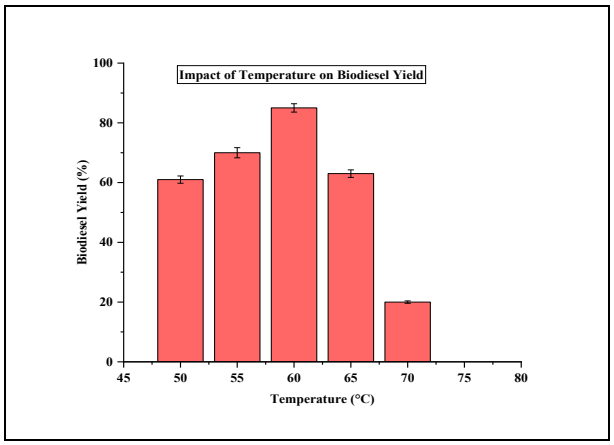


Fig. 5: Effect of temperature

3.2.1.3 Effect of Reaction Time

Various reaction times were investigated to determine their impact on enzymatic transesterification, ranging from 30 to 105 minutes in 15-minute intervals (Fig. 6). Using a lipase-immobilised biocatalyst, the optimal reaction time for converting cyanobacterial oil to fatty acid methyl esters was found to be 1 hour, yielding a maximum biodiesel conversion of approximately 88%. However, extending the reaction beyond this optimal duration resulted in a decline in lipase activity, likely due to the inhibitory effects of methanol and glycerol accumulation (Fukuda *et al.*, 2001).

3.2.1.4 Effect of Enzyme Loading

The effect of catalyst concentration on biodiesel production was investigated by varying the catalyst amount from 0.2 g to 1.0 g (Fig. 7), while maintaining a constant temperature of 60 °C, an agitation speed of 200 rpm, and a reaction time of 1 hour. The highest biodiesel yield of 88 % was achieved at a catalyst concentration of 0.6 g. Beyond this concentration, no significant improvement in yield was observed, likely due to saturation of active sites or mass transfer limitations. The

best balance between activity and cost was observed with 0.6 g of enzyme loading.

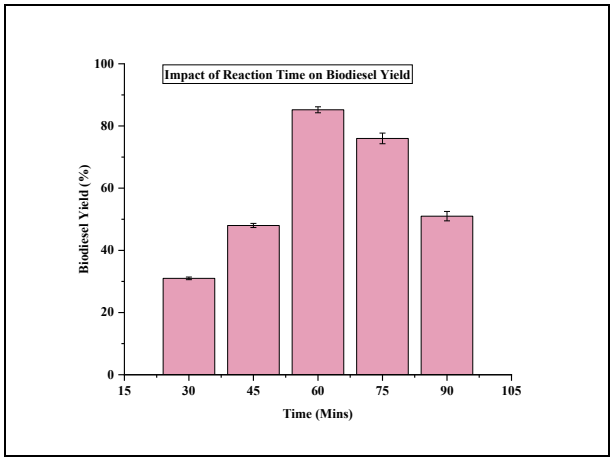


Fig. 6: Effect of reaction time

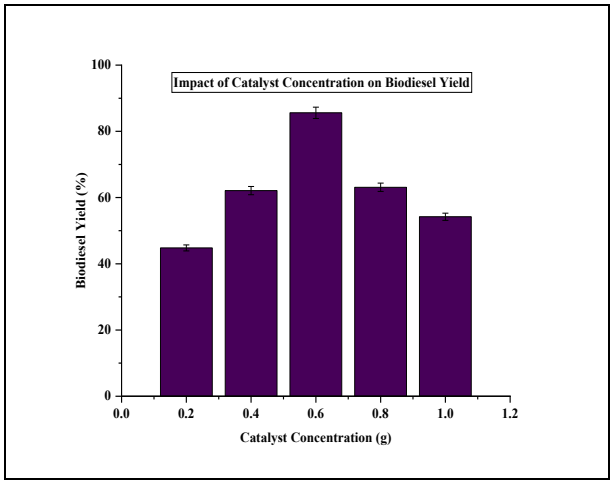


Fig. 7: Effect of enzyme concentration

3.2.1.5 Biodiesel Yield

Under optimised conditions, the immobilised lipase achieved a biodiesel yield of 88 %. Gas chromatographic analysis confirmed the formation of methyl esters as the primary product, with negligible amounts of free fatty acids remaining. Compared to free lipase, the immobilised enzyme showed a 15–20 % higher yield under the same conditions, attributed to enhanced stability and catalytic efficiency.

$$\text{Biodiesel yield (\%)} = \left(\frac{\text{weight of FAMEs}}{\text{weight of oil (g)}}\right) \times 100 \quad \ldots (1)$$

3.3 Reusability and Storage Stability

The immobilised nanobiocatalyst was evaluated over five consecutive reaction cycles. This gradual decline indicated good reusability, with 85% of the initial activity retained after the third cycle and 75% after the fifth (Fig. 8). The slight loss in activity was likely due to minor enzyme leaching and mechanical loss during recovery steps. Notably, the immobilised enzyme maintained structural integrity and continued to function effectively across multiple uses.

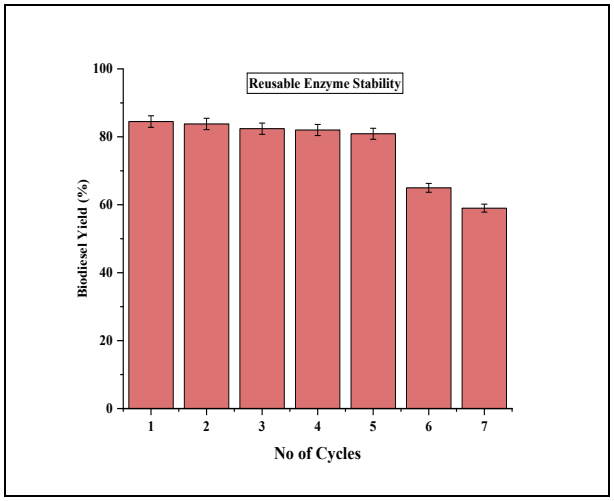


Fig. 8: Reusability and storage stability

3.4 Comparative Analysis

These results highlight the effectiveness of NiO nanoparticles in maintaining enzyme structure and function under reaction conditions. The approach offers a sustainable route for green biodiesel production by improving enzyme recovery and reducing process costs. Overall, the findings support the use of NiO-based enzyme immobilisation as a promising strategy for developing durable and efficient nanobiocatalysts in industrial biofuel applications.

Table 1. Comparative analysis of free and immobilised lipase enzyme

Parameter	Free Lipase	Immobilised Lipase
Optimal Temp. (°C)	35	60
Reaction Time (h)	30	1
Max Yield (%)	70	88
Reusability	None	5 cycles
Enzyme Recovery	Difficult	Easy (centrifugation)

3.5 Mechanistic Insight

The high surface area and reactive sites of NiO nanoparticles facilitate strong enzyme attachment, thereby reducing conformational mobility and enhancing thermal and operational stability. Furthermore, the nanoscale size promotes better substrate accessibility and diffusion, strengthening the overall reaction kinetics. This immobilisation strategy bridges the gap between homogeneous enzyme catalysis and heterogeneous

processing, enabling the green and scalable synthesis of biodiesel.

4. CONCLUSION

In this study, nickel oxide (NiO) nanoparticles were successfully synthesised and employed as an efficient support matrix for the covalent immobilisation of lipase derived from *Candida albicans*. Characterisation using XRD, FTIR, and SEM confirmed the crystalline nature, morphological integrity, and successful attachment of the enzyme to the nanoparticles. The nickel oxide nanoparticles exhibit a spherical shape, and the lipase enzyme is immobilised on the surface of the nickel oxide nanoparticles. The immobilised lipase demonstrated excellent catalytic activity in the transesterification of waste cooking oil, achieving a maximum biodiesel yield of 88% under optimised conditions. The nanobiocatalyst demonstrated notable thermal stability, retaining over 75% of its initial activity after five reuse cycles, which underscores its robustness and cost-effectiveness for industrial applications. The improved performance compared to free lipase can be attributed to the enhanced enzyme stability, better substrate accessibility, and ease of separation provided by the NiO nanoparticle matrix. These results highlight the potential of lipase-immobilised NiO nanoparticles as a green, sustainable, and scalable alternative for biodiesel production. Future studies may explore process intensification strategies, such as continuous-flow systems and magnetic recovery of catalysts, as well as their application to other renewable feedstocks, to further enhance the practicality and commercial viability of this approach.

FUNDING

This research received no specific grant from any funding agency in the public, commercial, or not-for-profit sectors.

CONFLICTS OF INTEREST

The authors declare that there is no conflict of interest.

ACKNOWLEDGEMENT

The authors are grateful to the Vellore Institute of Technology, Vellore, TN, India for providing the research facilities that enabled them to carry out the research work.

COPYRIGHT

This article is an open-access article distributed under the terms and conditions of the Creative Commons Attribution (CC-BY) license (http://creativecommons.org/licenses/by/4.0/).



REFERENCES

Abukhadra, M. R., Ibrahim, S. M., Yakout, S. M., El-Zaidy, M. E. and Abdeltawab, A. A., Synthesis of Na+ trapped bentonite/zeolite-P composite as a novel catalyst for effective production of biodiesel from palm oil; Effect of ultrasonic irradiation and mechanism, *Energy Convers. Manage.*, 196, 739–750 (2019). https://doi.org/10.1016/j.enconman.2019.06.027

Agarwal, P., Soni, R., Kaur, P., Madan, A., Mishra, R., Pandey, J., Singh, S. and Singh, G., Cyanobacteria as a Promising Alternative for Sustainable Environment: Synthesis of Biofuel and Biodegradable Plastics, *Front. Microbiol.*, *13* (2022). https://doi.org/10.3389/fmicb.2022.939347

Ali, M. A., Solanki, P. R., Patel, M. K., Dhayani, H., Agrawal, V. V., John, R. and Malhotra, B. D., *Nanoscale*, 5, 2883–2891 (2013). https://doi.org/10.1039/C3NR33459G

Basumatary, S., Nath, B. and Kalita, P., Application of agro-waste derived materials as heterogeneous base catalysts for biodiesel synthesis, *J. Renewable Sustainable Energy,* 10(4), 043105 (2018). https://doi.org/10.1063/1.5043328

Binsted, M., An electrified road to climate goals, *Nat. Energy,* 7 (1), 9-10 (2022). https://doi.org/10.1038/s41560-021-00974-8

Borges, M. E. and Díaz, L., Recent developments on heterogeneous catalysts for biodiesel production by oil esterification and transesterification reactions: a review, *Renew. Sustain. Energy Rev.,* 16 (5), 2839-2849 (2012). https://doi.org/10.1016/j.rser.2012.01.071

Chen, M. Z., Chen, L. P., Ma, Z., Xu, S., Hayat, T. and Alsaedi, A., Inflationary and distributional effects of fossil energy price fluctuation on the Chinese economy, *Energy,* 187, 115974 (2019). https://doi.org/10.1016/j.energy.2019.115974

Cherubini, F. and Strømman, A. H., Life cycle assessment of bioenergy systems: State of the art and future challenges, *Bioresour. Technol*., 102, 437–451 (2011). https://doi.org/10.1016/j.biortech.2010.08.010

Esmaeili, H., A critical review on the economic aspects and life cycle assessment of biodiesel production using heterogeneous nanocatalysts, *Fuel Process. Technol.,* 230, 107224 (2022). https://doi.org/10.1016/j.fuproc.2022.107224

Foster, E., Contestabile, M., Blazquez, J., Manzano, B., Workman, M. and Shah, N., The unstudied barriers to widespread renewable energy deployment: fossil fuel price responses, *Energy Policy*, 103, 258-264 (2017). https://doi.org/10.1016/j.enpol.2016.12.050

Fukuda, H., Konda, A. and Noda, N., Biodiesel fuel production by transesterification of oils, *J. Biosci. Bioeng.,* 92(5), 405-416 (2001). https://doi.org/10.1016/S1389-1723(01)80288-7

Garcia, R., Figueiredo, F., Brandão, M., Hegg, M., Castanheira, É., Malça, J., Nilsson, A. and Freire, F., A meta-analysis of the life cycle greenhouse gas balances of microalgae biodiesel, *Int. J. Life Cycle Assess.,* 25, 1737–1748 (2020). https://doi.org/10.1007/s11367-020-01780-2

Guerra, M. E. and Gude, V. G., Assessment of sustainability indicators for biodiesel production, *Appl. Sci.,* 7(9), 869-883 (2017). https://doi.org/10.3390/app7090869

Gui, M. M., Lee, K. T. and Bhatia, S., Feasibility of edible oil vs. non-edible oil vs. waste edible oil as biodiesel feedstock, *Energy*, 33(11), 1646-1653 (2008). https://doi.org/10.1016/j.energy.2008.06.002

Jambulingam, R., Shalma, M. and Shankar, V., Biodiesel production using lipase immobilised functionalized magnetic nanocatalyst from oleaginous fungal lipid, *J. Clean. Prod*., 215, 245–258 (2019). https://doi.org/10.1016/j.jclepro.2018.12.146

Joghee, S., Ganeshan, P., Alexramani, V., Sundrarajan, M. and Hong, I. S., Green synthesis and characterization of zinc oxide nanoparticle using insulin plant (Costus pictus D. Don) and investigation of its antimicrobial as well as anticancer activities, *Adv. Nat. Sci.: Nanosci. Nanotechnol.,* 9, 015008-015015(2018). https://doi.org/10.1088/2043-6254/aaa6f1

Kalita, P., Basumatary, B., Saikia, P., Das, B. and Basumatary, S., Biodiesel as renewable biofuel produced via enzyme-based catalyzed transesterification, *Energy Nexus*, 6, 100087 (2022). https://doi.org/10.1016/j.nexus.2022.100087

Koberg, M., Much, A. R. and Gedanken, A., Optimization of bio-diesel production from soybean and wastes of cooked oil; Combining dielectric microwave irradiation and a SrO catalyst, *Bioresour. Technol*., 102(2), 1073-1078 (2011). https://doi.org/10.1016/j.biortech.2010.08.055

Majhi, B. K., Cyanobacteria: Photosynthetic cell factories for biofuel production, *J. Bioresour. Bioprod.*, 10(2), 128–144 (2025). https://doi.org/10.1016/j.jobab.2024.10.001

Mercure, J. F., Salas, P., Vercoulen, P., Semieniuk, G., Lam, A., Pollitt, H., Holden, P. B., Vakilifard, N., Chewpreecha, U., Edwards, N. R. and Vinuales, J. E., Reframing incentives for climate policy action, *Nat. Energy*, 6 (12), 1133-1143 (2021). https://doi.org/10.1038/s41560-021-00934-2

Muthukumaran, C., Praniesh, R., Navamani, P., Swathi, R., Sharmila, G. and Kumar, N. M., Process optimization and kinetic modeling of biodiesel production using non-edible Madhuca indica oil, *Fuel,* 195, 217-225 (2017). https://doi.org/10.1016/j.fuel.2017.01.060

Nath, B., Das, B., Kalita, P. and Basumatary, S., Waste to value addition: Utilization of waste Brassica nigra plant-derived novel green heterogeneous base catalyst for effective synthesis of biodiesel, *J. Clean. Prod.,* 239, 118112 (2019). https://doi.org/10.1016/j.jclepro.2019.118112

Niasari, S. M., Ranjbar, M. and Mohandes, F., Self-assembly of cubic-like nanostructures to form star-like lead sulfatemicrostructures, *Micro and Nano Lett*., 7(6), 581–584 (2012). https://doi.org/10.1049/mnl.2012.0290

Okoye, P. U., Longoria, A., Sebastian, P. J., Wang, S., Li, S. and Hameed, B. H., A review on recent trends in reactor systems and azeotrope separation strategies for catalytic conversion of biodiesel-derived glycerol, *Sci. Total Environ.,* 719, 134595 (2020). https://doi.org/10.1016/j.scitotenv.2019.134595

Padilha, G. D. S., Santana, J. C. C., Alegre, R. M. and Tambourgi, E. B., Extraction of Lipase from Burkholderia cepacia by PEG/ Phosphate ATPS and its Biochemical Characterization, *Braz. Arch. Biol. Technol.,* 55(1), 7–19 (2012). https://doi.org/10.1590/S1516-89132012000100002

Parthiban, J. and Jambulingam, R., Enhancing the Biodiesel Production Potential of Synechococcus elongatus and Anabaena Cyanobacterial Strain Isolated from Saline Water Using Different Media Composition and Organic Carbon Sources, *Sustainability*, 15(1), 870 (2023). https://doi.org/10.3390/su15010870

Rajendran, S., Manoj, D., Raju, K., Dionysiou, Dionysios. D., Naushad, Mu., Gracia, F., Cornejo, L., Gracia-Pinilla, M. A. and Ahamad, T., Influence of mesoporous defect induced mixed-valent NiO (Ni^{2+}/Ni^{3+})-TiO_2 nanocomposite for non-enzymatic glucose biosensors, *Sens. Actuators, B*, 264, 27–37 (2018). https://doi.org/10.1016/j.snb.2018.02.165

Ramadhas, A. S., Jayaraj, S. and Muraleedharan, C., Biodiesel production from high FFA rubber seed oil, *Fuel*, 84 (4), 335-340 (2005). https://doi.org/10.1016/j.fuel.2004.09.016

Rawat, I., Kumar, R. R., Mutanda, T. and Bux, F., Biodiesel from microalgae: a critical evaluation from laboratory to large-scale production, *Appl. Energy*, 103, 444-467 (2013). https://doi.org/10.1016/j.apenergy.2012.10.004

Serio, M. D., Tesser, R., Pengmei, L. and Santacesaria, E., Heterogeneous catalysts for biodiesel production, *Energy Fuels*, 22 (1), 207-217 (2008). https://doi.org/10.1021/ef700250g

Sharma, Y. C. and Singh, B., Development of biodiesel: current scenario, *Renew. Sustain. Energy Rev*., 13(6-7), 1646-1651 (2009). https://doi.org/10.1016/j.rser.2008.08.009

Singh, A. R., Singh, S. K. and Jain, S., A review on bioenergy and biofuel production, *Mater. Today Proc.* 49, 510–516 (2021). https://doi.org/10.1016/j.matpr.2021.03.212

Sun, S. and Li, K., Biodiesel production from phoenix tree seed oil catalyzed by liquid lipozyme TL100L, *Renew. Energy,* 151, 152–160 (2020). https://doi.org/10.1016/j.renene.2019.11.006

Tayari, S., Abedi, R. and Rahi, A., Comparative assessment of engine performance and emissions fueled with three different biodiesel generations, *Renew. Energy,* 147, 1058–1069 (2020). https://doi.org/10.1016/j.renene.2019.09.068

Touqeer, T., Mumtaz, M. W. and Mukhtar, H., Lipase-Immobilized Magnetic Nanoparticles: Promising Nanobiocatalysts for Biodiesel Production, Nano- and Biocatalysts for Biodiesel Production*, John Wiley & Sons, Ltd*., 295–312 (2021). https://doi.org/10.1002/9781119729969.ch12

Vatanparast, M., Ranjbar, M., Ramezani, M. and Mashkani, H. S. M. and Kamazani, M. M., Sonochemical approach for synthesis and characterization of PbTe nanostructure, *Superlattices Microstruct.,* 65, 365–374 (2014). https://doi.org/10.1016/j.spmi.2013.10.042

Wang, Y., Zhu, J., Yang, X., Lu, L., and Wang, X., Preparation of NiO nanoparticles and their catalytic activity in the thermal decomposition of ammonium perchlorate, *Thermochim. Acta*, 437(1–2), 106–109 (2005). https://doi.org/10.1016/j.tca.2005.06.027

Wongsaprom, K. and Maensiri, S., Synthesis and room temperature magnetic behavior of nickel oxide nanocrystallites, *Ciang Mai J. Sci.,* 40(1), 99–108 (2013).

Xie, W. and Ma, N., Enzymatic transesterification of soybean oil by using immobilized lipase on magnetic nanoparticles, *Biomass Bioenergy*, 34(6), 890-896 (2010). https://doi.org/10.1016/j.renene.2019.11.006